THE JOURNAL OF BIOLOGICAL CHEMISTRY VOL. 282, NO. 14, pp. 10576–10584, April 6, 2007
Printed in the U.S.A.

Use of a cAMP BRET Sensor to Characterize a Novel Regulation of cAMP by the Sphingosine 1-Phosphate/G_{13} Pathway*[S]

Received for publication, October 16, 2006, and in revised form, January 29, 2007 Published, JBC Papers in Press, February 5, 2007, DOI 10.1074/jbc.M609695200

Lily I. Jiang[‡1], Julie Collins[‡], Richard Davis[‡], Keng-Mean Lin[‡], Dianne DeCamp[‡], Tamara Roach[§], Robert Hsueh[‡], Robert A. Rebres[§], Elliott M. Ross[‡], Ronald Taussig[‡], Iain Fraser[¶], and Paul C. Sternweis[‡2]

From the [‡]Department of Pharmacology, Alliance for Cellular Signaling, University of Texas Southwestern Medical Center, Dallas, Texas 75390-9196, the [§]Veterans Administration Medical Center, University of California, San Francisco, California 94121, and the [¶]Division of Biology, California Institute of Technology, Pasadena, California 91125

Regulation of intracellular cyclic adenosine 3′,5′-monophosphate (cAMP) is integral in mediating cell growth, cell differentiation, and immune responses in hematopoietic cells. To facilitate studies of cAMP regulation we developed a BRET (bioluminescence resonance energy transfer) sensor for cAMP, CAMYEL (cAMP sensor using YFP-Epac-RLuc), which can quantitatively and rapidly monitor intracellular concentrations of cAMP *in vivo*. This sensor was used to characterize three distinct pathways for modulation of cAMP synthesis stimulated by presumed G_s-dependent receptors for isoproterenol and prostaglandin E_2. Whereas two ligands, uridine 5′-diphosphate and complement C5a, appear to use known mechanisms for augmentation of cAMP via G_q/calcium and G_i, the action of sphingosine 1-phosphate (S1P) is novel. In these cells, S1P, a biologically active lysophospholipid, greatly enhances increases in intracellular cAMP triggered by the ligands for G_s-coupled receptors while having only a minimal effect by itself. The enhancement of cAMP by S1P is resistant to pertussis toxin and independent of intracellular calcium. Studies with RNAi and chemical perturbations demonstrate that the effect of S1P is mediated by the $S1P_2$ receptor and the heterotrimeric G_{13} protein. Thus in these macrophage cells, all four major classes of G proteins can regulate intracellular cAMP.

Cyclic adenosine 3′,5′-monophosphate (cAMP), a ubiquitous second messenger, mediates a wide range of cellular functions including cell metabolism (1), cell proliferation and differentiation (1), immune responses (2, 3), memory formation (4), and cardiac contractility (5). Canonically, the concentration of intracellular cAMP is regulated by two distinct families of enzymes. The transmembrane adenylyl cyclases (ACs)[3] synthesize cAMP from adenosine triphosphate (6, 7), whereas the cAMP-specific phosphodiesterases metabolize cAMP to biologically inactive adenosine 5′-monophosphate (8, 9). ACs are primarily activated by $G\alpha_s$ but their activities can also be differentially regulated by $G\alpha_i$, $G\beta\gamma$, or Ca^{2+} (10, 11). The activities of various phosphodiesterases can be regulated by protein kinase A (PKA), extracellular-regulated kinase (ERK), phosphoinositide 3-kinase, and the concentration of cAMP itself (12–16). Thus integration of signaling by stimuli that can regulate the intracellular concentration of cAMP will depend strongly on the various pathways and the subtypes of ACs and phosphodiesterases expressed in individual cells at any given time.

Assessment of the regulation of intracellular cAMP *in vivo* has only become possible recently. Zaccolo *et al.* (17) first described a FRET sensor for cAMP based on the cAMP binding domain of PKA. Subsequently, several reports have described FRET sensors for cAMP based on binding of the nucleotide to the Epac proteins (18–21). While these FRET sensors have been effective for measuring changes and localization of cAMP in single cells, measurements are tedious. Furthermore, the requirement for excitation of donor molecules produces a range of problems including cell damage, photobleaching, and low signal-to-noise ratios due to intrinsic cellular autofluorescence. This precludes use of the FRET sensors in high throughput population assays. In contrast, BRET (bioluminescence resonance energy transfer) sensors use an enzymatic reaction to produce energy emission in the donor, usually produce better signal-to-noise ratios, and are better suited for high throughput population assays (22). We report here the development and characterization of an Epac-based BRET sensor for cAMP (CAMYEL) with improved dynamic range and a method to quantify intracellular cAMP changes.

This sensor was further used to characterize a novel phenomenon identified in RAW 264.7 cells. The Alliance for Cellular Signaling (AfCS) has conducted a comprehensive double ligand screen using the mouse macrophage-like cell line, RAW

* This work was supported by National Institutes of Health Grant GM 62114, the Robert A. Welch foundation (to P. C. S.), and the Alfred and Mabel Gilman Chair in Molecular Pharmacology (to P. C. S.). The costs of publication of this article were defrayed in part by the payment of page charges. This article must therefore be hereby marked "*advertisement*" in accordance with 18 U.S.C. Section 1734 solely to indicate this fact.

[S] The on-line version of this article (available at http://www.jbc.org) contains supplemental data and Figs. S1–S7.

[1] To whom correspondence may be addressed: UT Southwestern Medical Center, 5323 Harry Hines Blvd, Dallas, TX 75390-9196. Tel.: 214-645-6105; Fax: 214-645-6118; E-mail: lily.jiang@utsouthwestern.edu.

[2] To whom correspondence may be addressed: UT Southwestern Medical Center, 5323 Harry Hines Blvd, Dallas, TX 75390-9196. Tel.: 214-645-6149; Fax: 214-645-6118; E-mail: paul.sternweis@utsouthwestern.edu.

[3] The abbreviations used are: AC, adenylyl cyclase; ISO, isoproterenol; PGE, prostaglandin E_2; C5a, complement C5a; S1P, sphingosine 1-phosphate; CAMYEL, cAMP sensor using YFP-Epac-RLuc; EIA, enzyme-linked immunoassay; TER, terbutaline; BRET, bioluminescence resonance energy transfer; FRET, fluorescence resonance energy transfer; RL, *Renilla* luciferase; SERCA, sarcoplasmic reticulum calcium ATPase; ERK, extracellular signal-regulated kinase; PKA, cAMP-dependent protein kinase.

264.7, to examine the extent of ligand interactions on a variety of downstream outputs, including cAMP (23). One of the striking results is the interaction between the lysophospholipid, sphingosine 1-phosphate (S1P), and ligands for receptors that stimulate cAMP. S1P alone does not significantly elevate either cAMP or Ca^{2+} in RAW 264.7 cells. However, S1P greatly increases the amount of intracellular cAMP stimulated by isoproterenol (ISO) and prostaglandin E_2 (PGE). Other ligands that stimulate mobilization of Ca^{2+} in RAW 264.7 cells, such as complement C5a and uridine 5′-diphosphate (UDP), also enhance stimulation of cAMP by ISO and PGE, but are less efficacious than S1P.

Receptors for S1P, formerly known as endothelial differentiation genes (Edg), are heptahelical transmembrane receptors that can variously interact with at least three G protein subfamilies, $G\alpha_i$, $G\alpha_q$, and $G\alpha_{12/13}$ (25–27), to affect regulation of phospholipase C ($G\alpha_i$ and $G\alpha_q$), phosphoinositide 3-kinase ($G\alpha_i$), and guanine nucleotide exchange factors for Rho ($G\alpha_{12/13}$) (28–33). S1P has also been shown to regulate inhibition of intracellular cAMP by a receptor-dependent $G\alpha_i$-mediated mechanism (29, 31, 32). Although S1P has been shown to stimulate intracellular cAMP in cells overexpressing S1P receptors, there is no evidence that the S1P receptors couple directly to $G\alpha_s$ and the mechanism remains unclear (30).

Using the CAMYEL sensor, we identified roles for $S1P_2$ receptors and G_{13} proteins in mediating the synergistic effect of S1P on cAMP responses. This is the first evidence that a G_{13} pathway is involved in the regulation of cAMP. Kinetic experiments indicate that the effect of S1P has rapid onset and works through increasing the rate of synthesis of the cyclic nucleotide.

EXPERIMENTAL PROCEDURES

Reagents—Isoproterenol, prostaglandin E_2, complement C5a, uridine 5′-diphosphate, 8-bromo cAMP, and phosphodiesterase inhibitors (Sigma), sphingosine 1-phosphate (Avanti Polar Lipids), terbutaline (Sigma), ICI 118551 (Biomol Research), SEW2871 (Cayman Chemical), and JTE 013 (Tocris bioscience) were purchased from the sources indicated.

DNA Constructs—Epac1 (amino acids 148–881) was generated by RT-PCR with human brain RNA as template using the primer pair 5′-CTC CGC GGA CCC GAG CCC GTG GGA ACT C-3′ and 5′-GTG AAT TCT GGC TCC AGC TCT CGG GAG AG-3′. Two point mutations, T781A and F782A, which eliminate the guanine nucleotide exchange activity of Epac (21), were created using site-directed mutagenesis with the QuikChange kit from Stratagene. Citrine with the monomeric mutation A206K and *Renilla* luciferase (RL) were amplified by PCR using primer pairs: 5′-ATG GAT CCA TGG TGA GCA AGG GCG AG-3′ and 5′-CCG CGG AGC TTG TAC AGC TCG TCC ATG-3′; 5′-GAA TTC ATG GCT TCC AAG GTG TAC G-3′ and 5′-GCG GCC GCT TAC TGC TCG TTC TTC AGC-3′. Fragments were then fused to the N and C termini of Epac1 as shown in Fig. 1. Circularly permuted citrine was generated by sewing PCR; constructs were equivalent to those described for the improved YFP, Venus (34). pcDNA3.1-His from Invitrogen was used for expression in mammalian cells; pQE30 from Qiagen was used for expression in bacteria. The pFB-neo vector from Stratagene was used to deliver the cAMP sensor into RAW 264.7 cells via retroviral infection.

Cell Culture and Transfection—Protocols for culturing RAW 264.7 cells and for transfection of DNA and siRNA or retroviral infection can be found at the AfCS website. Briefly, RAW 264.7 cells (obtained from ATCC) and HEK293 cells were cultured in Dulbecco's modified Eagle's medium supplemented with 10% fetal bovine serum, 2 mM L-glutamine, and 20 mM NaHEPES, pH 7.4. Transfection with DNA was carried out using Lipofectamine 2000 (Invitrogen) according to the manufacturer's protocol. Retrovirus was made with the Phoenix Amphotropic packaging cell line (Orbigen). Infection of RAW cells was initiated by applying virus-containing supernatant harvested from the packaging cell line with 6 μg/ml polybrene on top of the cells and spinning at 1,200 $\times$ *g* at 32 °C for 2 h. Cells were then cultured with the viral supernatant for 1 day at 32 °C followed by removal of the viral medium and further culturing with fresh medium containing 500 μg/ml G418 at 37 °C.

Gene Knockdown by RNAi—siRNA pools of oligomers targeting $S1P_1$, $S1P_2$, and $G\alpha_{13}$ were SMARTPool products purchased from Dharmacon. The sequence for the $S1P_2$-B oligomer (5′-GCA TGT CAC TCT GTC CTT A-3′) is unique from those in the SMARTPool. RAW cells were transfected with 400 nM siRNA using Lipofectamine 2000. Cells were plated into 96-well tissue culture plates at 24 h post-transfection and assayed at 48-h post-transfection. Samples were taken for Western blot or qRT-PCR to assess the knockdown level of protein or mRNA, respectively. Cells were lysed and blotted with antiserum B-860 to detect $G\alpha_{13}$ as described (35). Respective primers for qRT-PCR of the $S1P_1$ and $S1P_2$ receptors are: (F) 5′-CGG TGT AGA CCC AGA GTC CTG-3′ and (R) 5′-TTC TTT TAT GGA GCT TTT CCT TGG-3′; (F) 5′-AGC CAA CAG TCT CCA AAA CCA-3′ and (R) 5′-GGG CTG AGC ACT GGC TAG G-3′. The qRT-PCR reactions were done with an ABI 7500 Real-Time PCR system from Applied Biosystems.

EIA Assay for cAMP—Cells were plated on 96-well tissue culture plates 1 day prior to the treatment with ligands. Prior to treatments, cells were cultured in serum-free medium for 1 h. Ligands were then added to stimulate the cells. After the addition of ligands, reactions were stopped at the indicated times by removal of medium and cell lysis with 65% ethanol. Cell lysates were then dried and assayed using the cAMP Biotrak EIA kit (Amersham Biosciences).

Measurement of Fluorescence in Vitro—Cells that express the CAMYEL sensor were lysed with buffer containing 20 mM NaHEPES, pH 7.4, 50 mM KCl, 50 mM NaCl, 2.5 mM $MgCl_2$, 0.2% Nonidet P-40, 5 mM dithiothreitol, and a mixture of protease inhibitors (Roche Applied Science). Bacterial expressed protein with an N-terminal His_6 tag was purified with Ni-NTA resin. Coelenterazine-h (2 μM final concentration) was added to the cell lysates or purified proteins immediately prior to measurements of fluorescence emission spectra using a Spectrofluorometer MD-5020 (Photon Technology International).

Assay of BRET in Live Cells—Cells were plated in 96-well solid white tissue culture plates (Greiner) at a density of 60,000 cells per well the day before assays. Cells were serum-starved in Hank's balanced salt solution, pH 7.4, for 1 h before treatments. The BRET assay was carried out with a POLARstar Optima

plate reader from BMG LabTech. Emission signals from RL and YFP were measured simultaneously using a BRET[1] filter set (475–30/535–30). Cells in each well were assayed in 80 μl of Hank's balanced salt solution with 2 μM coelenterazine-h, and stimulations were initiated by injection of 20 μl of 5× ligand.

Calculation of cAMP Concentration—Ratiometric data were converted to cAMP concentration using Equation 1.

$$[\text{cAMP}] = K_d \times \left\{\frac{(R - R_{min})}{(R_{max} - R)}\right\} \quad \text{(Eq. 1)}$$

The K_d and Hill coefficient for association of cAMP with the sensor were determined to be 8.8 μM and 1, respectively. R is the intensity ratio of RL to YFP. R_{max} is obtained by adding 2 mM 8-bromo cAMP to the cells at the end of the assay. R_{min} is arbitrarily set to be the average ratio of measurements with unstimulated cells minus 4 S.D. (see supplementary data for details).

RESULTS

An Epac-based BRET Sensor for cAMP-CAMYEL—Several FRET sensors for detection of cAMP have been described in recent articles (19–21). Because the sensor containing an inactive cytosolic mutant form of human Epac-1 appeared to have the best signal-to-noise ratio (21), it was used as a basis for development of a BRET sensor. The design of the sensor is shown in Fig. 1*A*; it utilizes the enhanced variant of YFP, citrine (36), and *Renilla* luciferase as the BRET pair with human Epac1 inserted in between. Spectra of the expressed sensor protein revealed strong resonance energy transfer that was significantly reduced in response to cAMP, as expected from the FRET sensors and known structural changes in the molecule (21, 37, 38).

We sought to further improve the signal by replacing citrine with circularly permuted versions of the protein. Such circular permutations of the fluorescent proteins have been shown to vastly improve the FRET signal in a sensor for calcium (34). This improvement in FRET efficiency may be due to altered fluorophore orientation of the permuted proteins, and we reasoned that similar changes would apply to the efficiency of BRET sensors. Of the five different circular permutations screened, we found that replacement of citrine with citrine-cp229 improved the changes of BRET ratio upon binding cAMP by 2-fold (Fig. 1). The improved sensor gives an increase in BRET ratio (Rluc/YFP) of about 70% with cAMP and was named CAMYEL (cAMP sensor using YFP-Epac-RLuc).

The CAMYEL protein was expressed in bacteria and purified for further characterization. A concentration response analysis with cAMP indicated a K_d and n (Hill coefficient) for binding of 8.8 μM and 1, respectively (supplemental Fig. S1); these are similar to binding properties reported for the FRET sensor (21). While the activity of luciferase can be influenced by calcium, resonance energy transfer should be independent of these changes in absolute signals if calcium does not cause any conformational changes in the sensor protein. This appears to be the case because the BRET ratios, either in the presence or absence of cAMP, were not influenced by concentrations of calcium up to 1 mM (supplemental Fig. S2). Additional experiments indicated that the BRET signals were also independent of

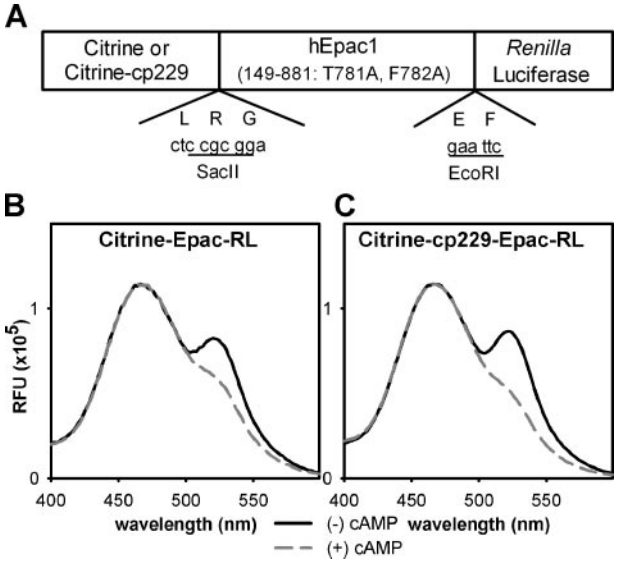

FIGURE 1. **An Epac-based BRET sensor for cAMP (CAMYEL).** *A*, schematic drawing of the domain structure of CAMYEL. The inactive cytosolic mutant form of human Epac-1 (amino acids 149–881, T781A, F782A) (21) was flanked by citrine or a circularly permuted citrine-cp229 and *Renilla* luciferase (*RL*). *B* and *C*, comparison of emission spectra of Citrine-Epac-RL (*B*) and Citrine-cp229-Epac-RL (*C*) in the presence and absence of 100 μM cAMP. HEK293 cells were transiently transfected with either construct. Cells were lysed with buffer containing 20 mM NaHEPES, pH 7.4, 50 mM KCl, 50 mM NaCl, 2.5 mM $MgCl_2$, 0.2% Nonidet P-40, 5 mM dithiothreitol, and protease inhibitors. Emission spectra were measured in the presence of 2 μM coelenterazine-h substrate with or without 100 μM cAMP.

changes in pH within the tested range (pH 6.5–8.0, supplemental Fig. S2). The response time of the sensor was assessed by measured changes in BRET when the sensor was exposed to abrupt increases or decreases in cAMP. Such changes depend on both the association and dissociation of cAMP and the ensuing changes in conformation. *In vitro*, the change of BRET ratio in response to altered cAMP concentrations appears to be complete within 1 to 2 s (supplemental Fig. S3). This rate of signal change is well suited for measuring the kinetics of change in intracellular concentrations of cAMP.

Regulation of Cytosolic cAMP in RAW 264.7 Cells—One of the outputs measured in a survey by the Alliance for Cellular Signaling for the complexity of interactions among signaling pathways was the regulation of the classical second messenger, cAMP. A traditional enzyme-linked immunoassay (EIA) for total intracellular cAMP was used to identify two ligands, isoproterenol (ISO) and prostaglandin E_2 (PGE), which effectively increased this second messenger in RAW cells. These two ligands were subjected to a comprehensive double ligand screen with over twenty additional ligands to look for non-additive interactions (23). Ligands that elicit calcium responses in RAW cells, such as complement C5a and uridine 5′-diphosphate (UDP), enhanced cAMP responses triggered by ISO or PGE. Interestingly, S1P, which at best induced only minimal cAMP or calcium responses in RAW cells by itself, enhanced the cAMP response to the ISO or PGE by 2–3-fold (Fig. 2*A*). To study these synergistic interactions in detail, cell lines that stably express the sensor for cytosolic cAMP, CAMYEL, were derived from RAW 264.7 cells. The level of expression of the CAMYEL sensor in the RAW 264.7 cells was estimated to be about 100 nM based on comparative Western blots. These cells

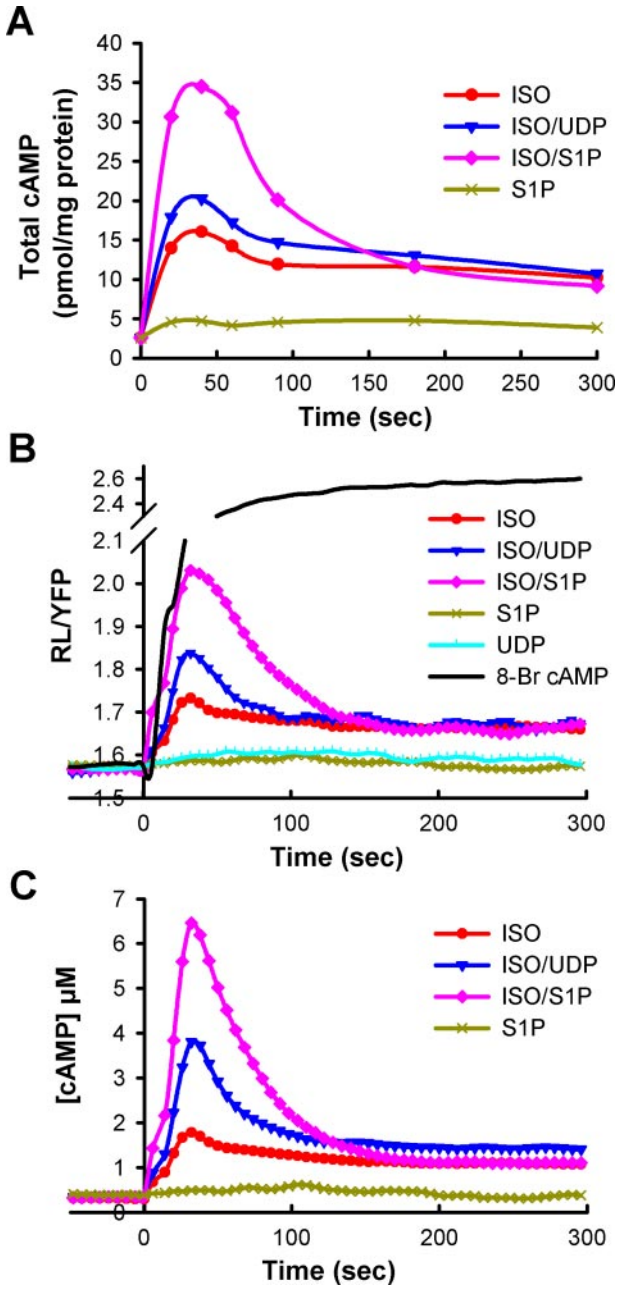

FIGURE 2. **Measurement of intracellular cAMP responses in RAW 264.7 cells.** *A*, changes in cAMP measured by EIA. At time 0, cells were stimulated with16 nM ISO, 16 nM ISO and 0.5 μM UDP, 16 nM ISO and 10 nM S1P, or 50 nM S1P as indicated. At the given times, reactions were stopped by removal of medium and addition of cell lysis solution, and cAMP was determined by EIA. The results shown are the average of three independent experiments done with two different preparations of cells: the variance among the experiments is about 30% of the signals. *B*, measurement of cAMP responses using the CAMYEL sensor. Emission ratios (RL/YFP) were measured in RAW 264.7 cells stably expressing the CAMYEL sensor. Cells were stimulated at time 0 by addition of either 16 nM ISO 16 nM ISO and 0.5 μM UDP, 16 nM ISO and 10 nM S1P, 10 nM S1P, 2.5 μM UDP, or 2 mM 8-bromo cAMP as indicated. *C*, ratiometric measurements of CAMYEL responses were converted to intracellular concentrations of cAMP.

produced normal calcium and cAMP (as measured by EIA) responses to an array of ligands. In such cell lines the BRET ratio, RLuc/YFP, can then be used to continuously monitor intracellular cAMP in real time (Fig. 2*B*). The dynamic range of the sensor in RAW cells was measured using 2 mM 8-bromo cAMP, a cell-permeable analog of cAMP, to saturate the sensor *in vivo*.

Stimulation of β-adrenergic receptors with ISO led to rapid decreases of the BRET signal hence increases of the fluorescence intensity ratio, Rluc/YFP (Fig. 2*B*). The response peaked at ~20–30 s after addition of ligand and declined to a sustained level. This response profile is qualitatively the same as measured by EIA. The BRET sensor also recapitulates the effect of S1P and UDP on production of cAMP. Addition of either S1P or UDP alone elicited minimal cAMP responses (Fig. 2*B*), although UDP stimulates robust increases in intracellular calcium in RAW cells. This confirms *in vitro* results that calcium does not affect the BRET ratio of the sensor. Simultaneous addition of either S1P or UDP together with ISO led to greater changes in BRET at the peak of the response and subsequent decreases over time to a sustained level that was equivalent to that obtained with the addition of ISO alone.

To better assess the dynamics of changes in intracellular cAMP, we converted the ratiometric results shown in Fig. 2*B* to concentrations of cAMP (Fig. 2*C*, see "Experimental Procedures" and supplementary information). Using this method of conversion, we can then compare quantitative changes in cAMP measured with the BRET sensor to those obtained with the EIA. As shown in Fig. 2*C*, S1P or UDP synergistically increases the peak cAMP response induced by ISO alone by 2–4 or 1.5–2 folds, respectively. This slightly higher ratio of enhancement than that observed with EIA is likely due to two differences in the assessments. First, the peak response is usually missed by the EIA. Second, the sensor measures free intracellular cAMP, whereas the EIA also measures bound nucleotide that will be proportionally higher at lower concentrations.

Enhancement of cAMP by S1P Is Caused by Increased Synthesis of cAMP—Use of the CAMYEL sensor allows us to dissect the effect of S1P on cAMP through detailed kinetic measurements. The intracellular concentration of cAMP is determined by a dynamic balance between its biosynthesis via adenylyl cyclases and its degradation by phosphodiesterases. The enhancement observed with S1P could be due to either stimulation of synthesis or inhibition of degradation. We first compared rates of cAMP increases when cells were stimulated by either ISO alone or combination of ISO and S1P. The synergistic effect of S1P is observed at the earliest times after ligand addition with a greater than 4-fold increase in rate throughout the approach to peak values (Fig. 3, *filled symbols*). This suggests that the enhancement by S1P is temporally well-coupled to the early processes causing activation of ACs.

Inhibitors of phosphodiesterases were then used to reduce degradation of cAMP. Under these conditions, ISO produced a much greater rise in intracellular cAMP, which was readily sustained over longer times. However, blocking degradation of cAMP did not reduce the enhanced rate or the extent of cAMP accumulation affected by S1P (Fig. 3, *open symbols*). Similar results were obtained with PGE, and its combination with S1P (data not shown). These results clearly indicate that modulation of phosphodiesterase activity is not a primary mechanism by which S1P enhances cAMP.

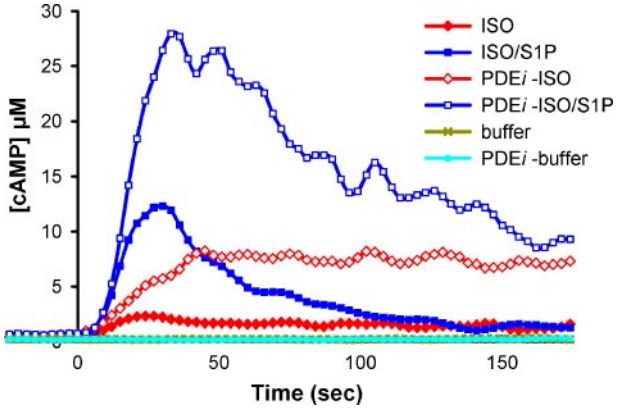

FIGURE 3. **Effect of S1P on intracellular cAMP has a fast onset and is not affected by inhibitors of phosphodiesterases.** The CAMYEL sensor was used to measure the rise in cAMP when cells were treated with 16 nM ISO or 16 nM ISO and 10 nM S1P either in the absence or in the presence of the phosphodiesterase inhibitors (*PDEi*), 10 μM Ro20–1724 and 40 μM isobutylmethylxanthine. Ligands were added at time 0, PDEi were added 2 min prior to ligand addition, which was sufficient to cause maximum impact of the inhibitors.

Stimulation of cAMP by S1P Is Related to the Activities of the G_s Pathway—When RAW cells expressing the CAMYEL sensor are treated with ISO, the cells rapidly increase the level of free intracellular cAMP to a peak response (~20–30 s); this is usually followed by a rapid decrease to a sustained response that declines slowly over time. To examine the temporal coupling between the effect of S1P and activation of the G_s pathway, S1P was added either simultaneously with ISO or during the sustained phase of the ISO response (Fig. 4*A*). Interestingly, the synergistic effect of S1P on intracellular cAMP was observed throughout the experiment. Moreover, the increase in cAMP induced by addition of S1P is directly related to the concentration of intracellular cAMP stimulated by ISO at the time of S1P addition (Fig. 4*B*). Thus, the relative enhancement by S1P, a maximal increase of about 300% over the stimulation produced by ISO alone, remained the same regardless of when the ligand was added after ISO. This indicates that not only can S1P exert its effect as long as the synthetic pathway for cAMP is active, but also the mechanism for the effect of S1P is not altered by the magnitude of cAMP synthesis activated by GPCR-G_s pathways.

The dependence of the S1P effect on the synthetic pathway of cAMP was further tested by termination of stimulation of the β-adrenergic receptor with a specific antagonist, ICI-118551. For this study, the agonist terbutaline (TER), which has a lower affinity and faster rate of dissociation than ISO, was used. As shown in Fig. 4*C*, S1P enhanced the cAMP response triggered by TER as it did to that of ISO. Addition of ICI-118551 led to a rapid decline of intracellular cAMP that had been stimulated by TER (*green trace*, *inverted triangles*). Simultaneous addition of ICI-118551 and S1P greatly reduced the effect of S1P in tandem with inhibition of TER although transient enhancement was observed (*red trace*, *open circles*). If the addition of ICI-118551 preceded that of S1P by 12 s, the effect of S1P was abolished (*green trace*, *inverted triangles*). Therefore the S1P effect requires activation of the $G\alpha_s$ pathway and adenylyl cyclase. Because the adenylyl cyclase activity in the RAW cells is unresponsive to forskolin, a simple requirement for active adenylyl cyclase could not be tested.

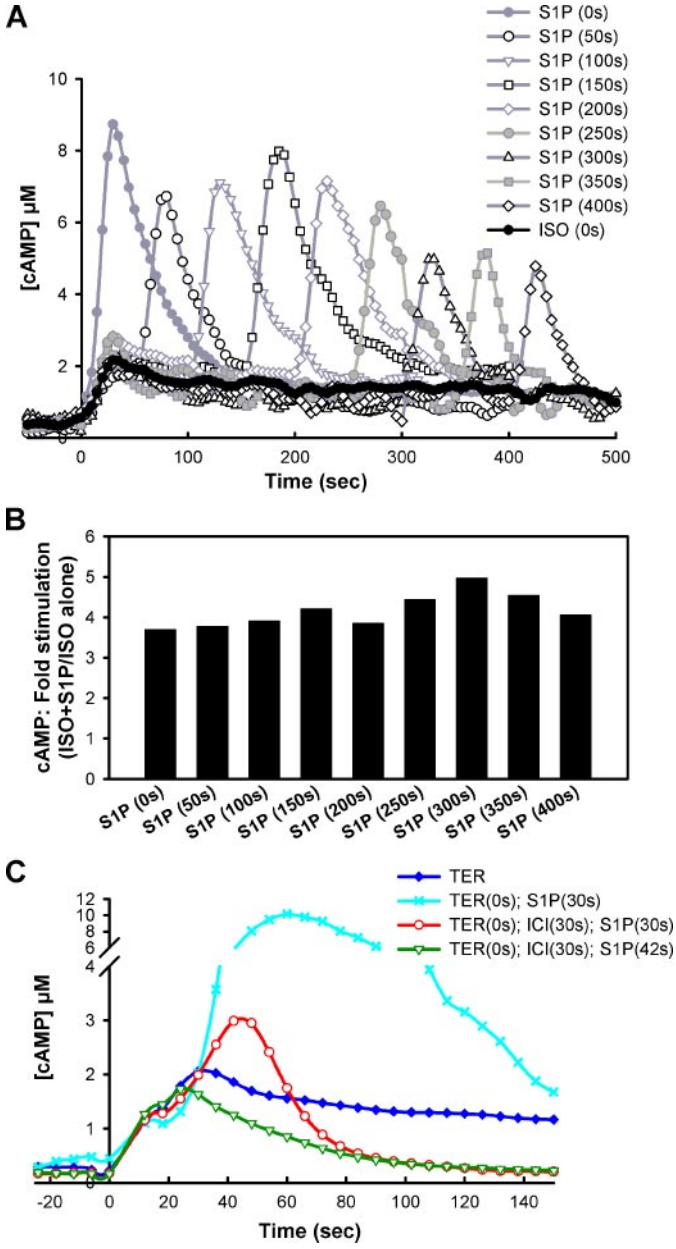

FIGURE 4. **Effect of S1P on cAMP parallels activation of G_s.** *A*, changes in cAMP were measured with CAMYEL; cells were treated with 16 nM ISO at time 0 followed by addition of 10 nM S1P at the indicated times. *B*, effect of S1P on intracellular cAMP is expressed as the ratio of the S1P induced peak of cAMP to the concentration of cAMP induced by ISO alone at the time of S1P addition. For simultaneous addition of ISO and S1P the ratio is calculated as the peak induced by the two ligands *versus* that by ISO alone. The synergistic effect of S1P on cAMP appears to be the same throughout the 7 min assay period. *C*, termination of β-adrenergic receptor signaling diminished the effect of S1P. All cells were treated with 2.5 μM TER at time 0. Addition of 10 nM S1P at 30 s greatly enhanced the cAMP response stimulated by TER (*cyan*, x). Simultaneous addition of 10 nM S1P and 10 μM ICI 118551 (*ICI*), a β-adrenergic antagonist, greatly reduced the ability of S1P to affect increases in cAMP (*red*, ○). Addition of 10 μM ICI 118551 at 30 s immediately initiated a decline in cAMP; subsequent addition of 10 nM S1P 12 s later produced no effect on intracellular cAMP concentration (*green*, ▽).

Enhancement of cAMP by UDP and C5a Is Mediated by Calcium and G_i Pathways, Respectively—The activity of adenylyl cyclases can be regulated by calcium and the G_i pathway (11). To examine the role of calcium in the enhancements of cAMP by UDP, C5a, and S1P, intracellular and extracellular calcium

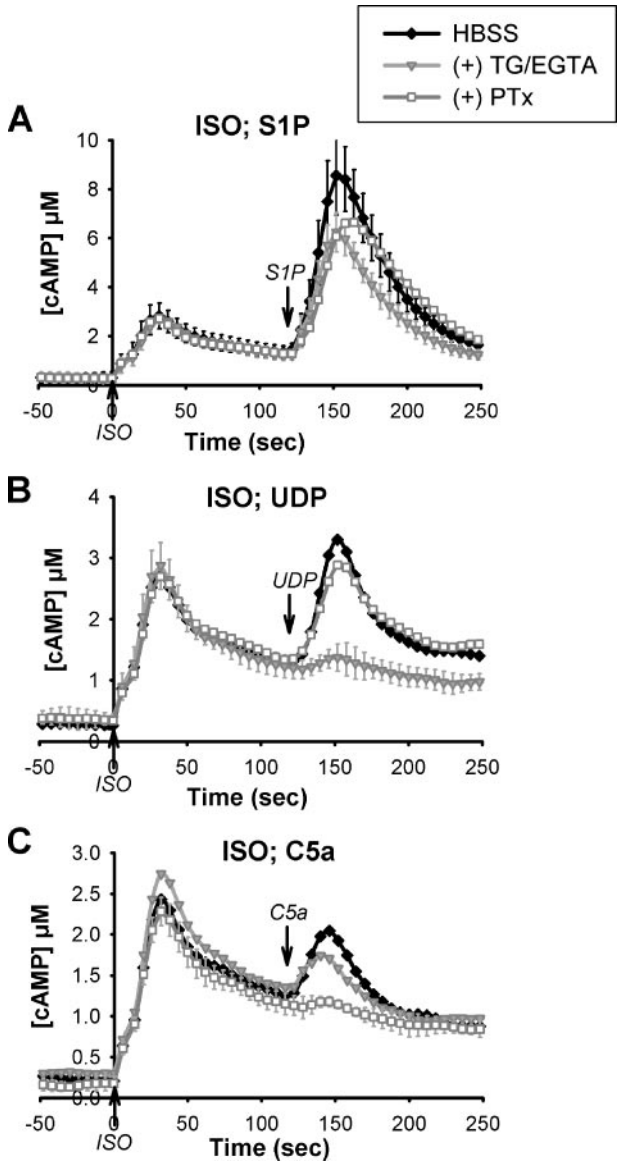

FIGURE 5. **Effect of intracellular calcium and activity of the G_i pathway on cAMP responses to dual ligands in RAW 264.7 cells.** Cells expressing the CAMYEL sensor were treated with 50 ng/ml pertussis toxin for 20 h or 1 μM thapsigargin and 2 mM EGTA for 2 min as indicated prior to ligand additions. cAMP responses were induced by addition of 16 nM ISO at time 0 followed by addition of 10 nM S1P (*A*), 0.5 μM UDP (*B*), or 100 nM C5a (*C*). Results shown are averages from at least three experiments, *error bars* represent the S.D.

were depleted by addition of the SERCA inhibitor thapsigargin and calcium chelator EGTA. The synergistic effects of S1P, UDP or C5a on cAMP responses induced by ISO were assessed with a sequential ligand format where addition of the enhancing ligands triggers a second peak response after the initial response of cAMP to ISO (Fig. 5). Attenuation of intracellular calcium did not affect the first cAMP response peak induced by ISO, nor did it significantly affect the second peak response triggered by S1P or C5a (Fig. 5, *A* and *C*). However, the enhancement by UDP was largely ablated without intracellular calcium (Fig. 5*B*).

Inactivation of the G_i pathway was achieved by treatment of the cells with pertussis toxin. As shown in Fig. 5, inactivation of the G_i pathway effectively ablated the effect of C5a on cAMP without significantly affecting the cAMP response of ISO alone (Fig. 5*C*) or the synergistic effects of UDP and S1P (Fig. 5, *A* and *B*). In contrast to UDP and C5a, the stimulation of cAMP observed with S1P could not be explained by these known mechanisms.

The $S1P_2$ Receptor Mediates the Changes in cAMP Caused by S1P—RAW 264.7 cells express two receptors for sphingosine 1-phosphate, $S1P_1$ (Edg1) and $S1P_2$ (Edg5), as determined by RT-PCR. A knockdown approach with RNAi was used to determine which receptor is responsible for mediating the effect of S1P. Pools of four different siRNA oligomers specifically targeting either $S1P_1$ or $S1P_2$ were transfected into RAW cells carrying the CAMYEL sensor. The effects of gene specific knockdown were assessed by qRT-PCR (Fig. 6*A*). Knockdown of the $S1P_2$ receptor greatly reduced the synergistic effect of S1P without changing the cAMP response triggered by ISO alone. This phenotype is evident with either simultaneous addition of ISO and S1P (Fig. 6*C*) or sequential addition of ISO followed by S1P (Fig. 6*D*). A single siRNA oligomer ($S1P_2$-B) that targets $S1P_2$ was selected independently of the oligomer pool and used to confirm the specificity of the $S1P_2$ knockdown phenotype (Fig. 6*D*). A partial knockdown of $S1P_1$ appeared to slightly enhance the synergistic response of cAMP to S1P. However, the enhancing effect appeared to be nonspecific as an increase was also observed when the cells were stimulated with the combination of ISO and UDP (Fig. 6*B*).

The receptor knockdown result was further confirmed by drug perturbations. SEW2871 is an agonist for the $S1P_1$ receptor (39). Addition of SEW2871 following that of ISO failed to reproduce the effect of S1P (Fig. 6*E*). However, addition of JTE-013, an antagonist for the $S1P_2$ receptor (40), at 12 s prior to S1P addition greatly reduced the effect of S1P on the cAMP response triggered by ISO (Fig. 6*F*). Together these results indicate that S1P preferentially uses the $S1P_2$ receptor to enhance intracellular concentrations of cAMP in RAW cells.

Stimulation of cAMP by S1P Is Mediated by $G\alpha_{13}$—Whereas $S1P_1$ is reported to couple primarily to G_i (31, 32), $S1P_2$ can act through G_i, G_q, and $G_{12/13}$ to stimulate a variety of pathways (30, 31, 33). Because inactivation of the G_i pathway did not attenuate the S1P effect on cAMP and the lack of calcium response to S1P indicates that activation of G_q is unlikely, we explored the potential role of G_{13} in the S1P synergism. As shown in Fig. 7, transfection of cells expressing the CAMYEL sensor with siRNAs targeting $G\alpha_{13}$ greatly reduced the enhancement of S1P on the cAMP response generated by ISO (Fig. 7, *C* and *D*). In contrast, the response of cAMP to ISO alone or its enhancement by UDP, a ligand which likely acts through a G_q-coupled mechanism, remained unaffected (Fig. 7*B*). The enhanced effect of S1P on the cAMP response of PGE was also attenuated by the knockdown of $G\alpha_{13}$ (Fig. 7*E*).

The specificity of $G\alpha_{13}$ involvement in the S1P synergy on cAMP was assured by using a micro-RNA based shRNA delivered via retroviral infection to knockdown $G\alpha_{13}$. The targeting sequence was selected independently of the pooled oligomers, and a similar phenotype was observed when cAMP was measured either with the CAMYEL sensor or an EIA (supplemental Fig. S5). The partial reduction of the response is consistent with an incomplete knockdown of the $G\alpha_{13}$, but could also be indic-

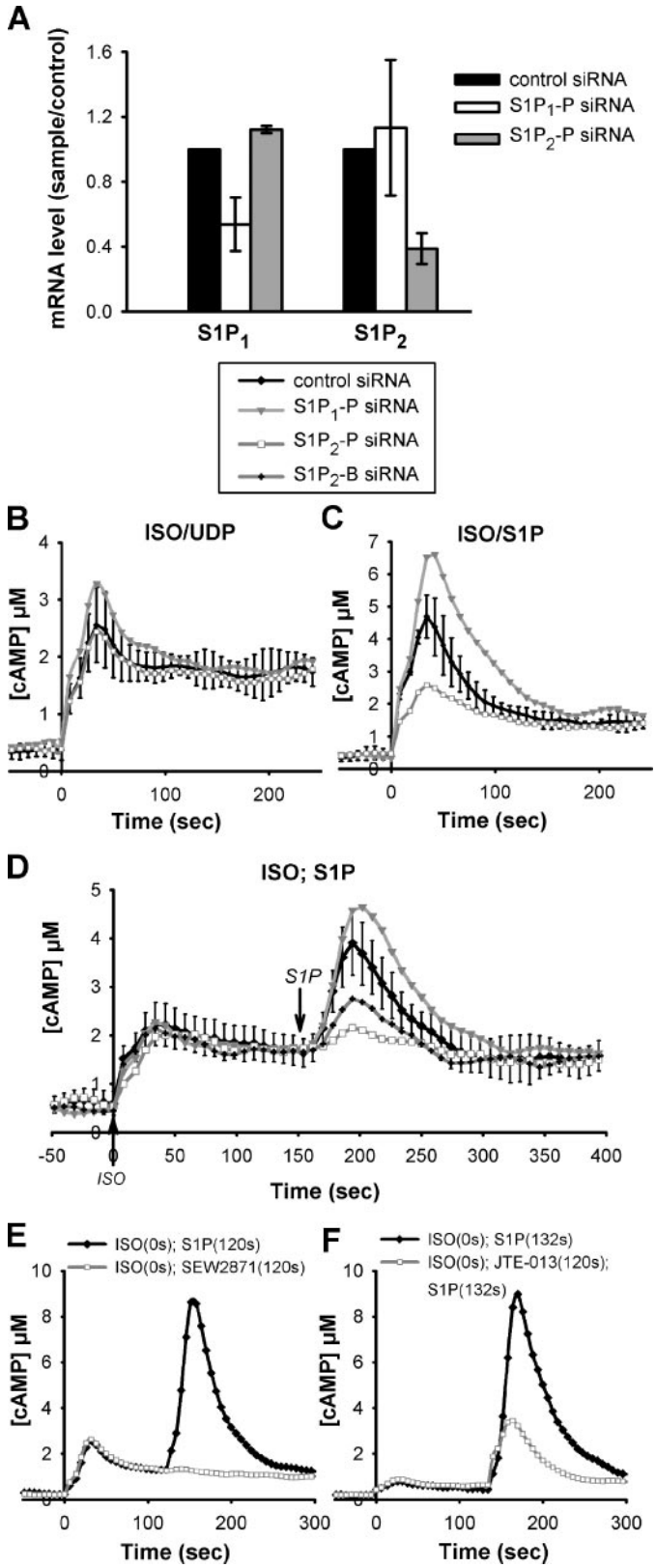

FIGURE 6. **The $S1P_2$ receptor transduces signaling by S1P for modulation of intracellular cAMP.** *A*, RAW cells expressing CAMYEL were transiently transfected with control siRNA or pools of four siRNA oligomers (designated as *–P*) targeting either the $S1P_1$ or $S1P_2$ receptor. Analysis by qRT-PCR showed specific but partial knockdowns of the $S1P_1$ and $S1P_2$ receptors. *B–D*, cells were assayed for cAMP responses to simultaneous addition of 16 nM ISO and 0.5 μM UDP (*B*), simultaneous addition of 16 nM ISO and 10 nM S1P (*C*), and sequential addition of 16 nM ISO followed by 10 nM S1P (*D*). Knockdown of $S1P_2$ using a single oligomer ($S1P_2$-B) that is independent of the pool of four oligomers resulted in a similar phenotype (*D*). *E*, addition of 1 μM SEW2871, an agonist for the $S1P_1$ receptor, at 2 min after addition of ISO failed to induce a synergistic cAMP response. *F*, addition of 100 nM JTE-013, an antagonist of $S1P_2$ receptors, at 12 s prior to addition of S1P significantly reduced the synergistic effect on cAMP. Ligands were added at time 0 or as indicated. *Error bars* represent the S.D. of results from four experiments of 2 independent transfections. Errors were similar for the other traces but left out for clarity.

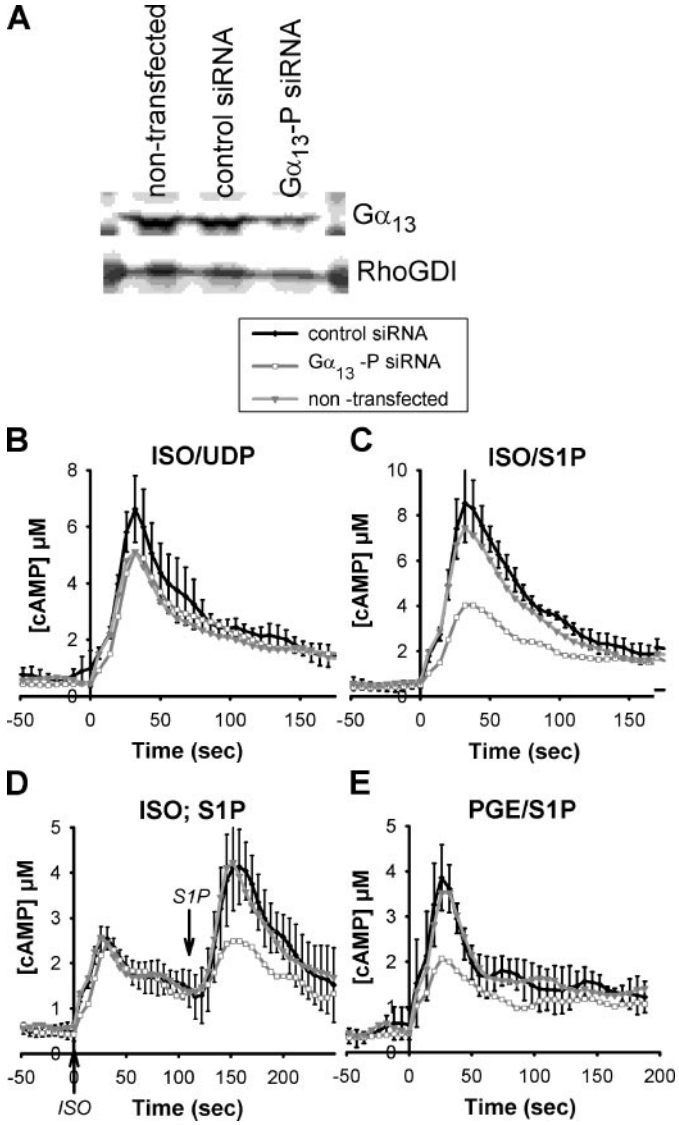

FIGURE 7. **$G\alpha_{13}$ is required for the synergy of S1P on G_s-mediated cAMP responses.** *A*, RAW cells expressing CAMYEL were transiently transfected with control siRNA or a pool of four siRNA oligomers (designated as *–P*) specifically targeting $G\alpha_{13}$. The presence of $G\alpha_{13}$ was assessed by Western blot. The reduction of the α-subunit in cells treated with four siRNA oligomers targeting $G\alpha_{13}$ was about 60%. *B–D*, response of cAMP in control transfected and $G\alpha_{13}$ knockdown cells to simultaneous addition of 16 nM ISO and 0.5 μM UDP (*B*), simultaneous addition of 16 nM ISO and 10 nM S1P (*C*), and sequential addition of 16 nM ISO followed by 10 nM S1P (*D*). *E*, synergy of S1P on intracellular cAMP induced by PGE is also reduced in $G\alpha_{13}$ knockdown cells. Ligands were added at time 0 or as indicated. *Error bars* represent the standard deviation of results from four experiments of 2 independent transfections. Errors were similar for the other traces but left out for clarity.

ative of contributions from a second pathway. Attempts to assess potential involvement of the most obvious candidate, $G\alpha_{12}$, have been hampered by our inability to produce effective knockdown of this α subunit in RAW cells.

DISCUSSION

We successfully converted an Epac-based FRET sensor for cAMP to a BRET sensor. The signal of the new sensor was improved 2-fold by using circularly permuted fluorescent proteins, a technological advance used previously to alter the efficiency of resonance energy transfer between FRET pairs (34). The use of circularly permuted citrine in CAMYEL demonstrates the utility of this method for evolving better sensors using bioluminescent donors as well. With its good signal-to-noise ratio and excellent dynamic range, CAMYEL is ideal for continuous *in vivo* monitoring of cAMP metabolism in populations of cells.

The use of permeable cAMP analogs to saturate output further allows calibration of the sensor and conversion of ratiometric measurements to real estimates of cAMP concentration. Its rapid and reversible response makes the sensor an excellent tool to measure the kinetics of this signaling pathway and hence support molecular modeling of this signaling system, one of the goals of the Alliance for Cellular Signaling. The use of CAMYEL for exploring regulation of signaling pathways is described herein. The sensor also has the potential to support high throughput genome-wide genetic screens, such as an RNAi screen, to identify new players involved in the regulation of cAMP as well as screens for small molecule drugs.

The BRET sensor was used to characterize the cAMP responses to dual ligands in mouse macrophage-like RAW 264.7 cells. Three ligands, which do not stimulate cAMP by themselves, were found to enhance production of cAMP induced by G_s-coupled receptors via three distinct mechanisms. The effects of UDP and C5a on cAMP responses are likely due to canonical regulation of adenylyl cyclase activity via calcium regulated by G_q proteins and the G_i pathway, respectively. Interestingly, the ability of S1P to enhance cAMP production stimulated by G_s-coupled ligands uses neither of these known pathways. Rather, S1P acts through $S1P_2$ receptors and uses the heterotrimeric G_{13} proteins to couple to the synthesis of cAMP. This is the first evidence that a member of the $G_{12/13}$ subclass of G proteins can robustly regulate production of this classic and ubiquitous second messenger.

One remaining issue is to identify the site of action for stimulation of cAMP synthesis by the S1P/G_{13} pathway. Three possible sites of action are the stimulatory receptors, G_s, or direct action on adenylyl cyclases. Enhancement of the action of β-adrenergic receptors on G_s, perhaps facilitated by oligomerization of receptors or modification of receptors, would likely be accompanied by a shift in the concentration response curve of ISO to a lower EC_{50} in the presence of S1P. However, the EC_{50} of the ISO response remained the same, regardless of S1P (supplemental Fig. S4). In addition, the S1P/G_{13} pathway also synergistically stimulates cAMP triggered by PGE. This would require the S1P/G_{13} pathway to somehow couple with both the β-adrenergic and prostaglandin receptors. Enhancement of the activity of G_s by the S1P/G_{13} pathway would require pre-activation of G_s as S1P by itself does not activate G_s. Examples of such regulation are not known but mechanisms might include inhibition of the GTPase activity of $G\alpha_s$ in analogy to the action of cholera toxin. This seems unlikely because the G_s pathway is common to all cells and this enhancement of cAMP synthesis by S1P/G_{13} is not observed in many other cells (such as HEK293 and HeLa) where S1P activates G_{13} (data not shown). The most likely target is one or more subtypes of adenylyl cyclase, because specific subtypes have already been described that account for the impact of calcium and G_i. RAW 264.7 cells minimally express four adenylyl cyclases, AC2, AC3, AC7, and AC9, where AC2 could account for the G_i-dependent effects of C5a via a $\beta\gamma$ mechanism and AC3 could respond to stimulation via calcium/calmodulin. We are in the process of determining the role of each of these cyclase subtypes in the cAMP response of RAW cells to hormonal stimuli.

A hint to the mechanism of S1P synergy may be evident in the brief but significant increase in cAMP when S1P and the β-adrenergic antagonist were added to cells stimulated with TER (Fig. 4*C*). In the absence of S1P, the antagonist initiates an almost immediate decline in cAMP, suggesting rapid dissociation of TER from the receptor and coincident inactivation of the receptor and adenylyl cyclase. When S1P was added simultaneously with the antagonist, there was an immediate increase in cAMP that lasted about 10 s before the second messenger started to decline. This indicates that adenylyl cyclase was not rapidly inactivated under this condition and suggests S1P can act rapidly by some mechanism to increase the lifetime of activated adenylyl cyclase, either by itself or in complex with G_s.

How does the G_{13} pathway regulate cAMP synthesis? Conceivably, release of the $\beta\gamma$ subunits from G_{13} could account for the enhancing activity of S1P in a fashion similar to that of $\beta\gamma$ subunits released from G_i to regulate the activity of ACs (10, 11, 41, 42). Alternatively, $G\alpha_{13}$ could act directly on adenylyl cyclase. No evidence for this has yet been generated in attempts to reconstitute the phenomena with cellular membranes and activated $G\alpha_{13}$ proteins (data not shown). A well-characterized pathway stimulated by G_{13} is Rho-dependent regulation of cytoskeleton and gene transcription (43, 44). We used inhibitors of Rho and Rho kinases to block this pathway but failed to disrupt the S1P synergy (supplemental Fig. S6). At this time, further elucidation of mechanism will likely require identification of additional players in the pathway. Use of the CAMYEL sensor makes it possible to screen for such a player in a genome-wide high throughput fashion.

What is the physiological relevance of this S1P/G_{13} effect in intracellular cAMP regulation? To begin answering this question, we examined the cAMP responses in primary macrophages derived from mouse bone marrow. The application of S1P robustly enhanced the stimulation of cAMP production observed with agonists of G_s-coupled receptors and its effect appears to be prolonged into the sustained phase of the cAMP response (supplemental Fig. S7). Interestingly, a similar phenomenon of enhancement on cAMP responses has been reported for thrombin in a human erythroleukemia cell line and human erythroid progenitor cells (45–47). In both cell lines, thrombin does not trigger either cAMP or calcium responses on its own, yet it can potentiate G_s-activated increases in intracellular cAMP. A mechanism for this effect of thrombin was not reported. Regulation of cAMP plays an important role in cell growth, differentiation, and cellular functions in the immune system. Both S1P and thrombin are also known to modulate

immune responses in various hematopoietic cells (24, 26). Conceivably, the ability of other GPCR pathways to enhance intracellular cAMP responses may help reinforce certain cellular responses or lead to concerted cellular behaviors. It will be of interest to determine the downstream targets of enhanced cAMP responses and their effect on cellular function and immune function in animals. For example, a major function of macrophage cells is to produce and release cytokines upon activation; these processes are strongly modulated by cAMP in the RAW macrophages and currently under investigation by the AfCS.

Acknowledgments—We thank Jana Hadas for help with protein purification and Drs. William Singer and Scott Gibson for plasmids.

REFERENCES

1. Lania, A., Mantovani, G., and Spada, A. (2001) *Eur. J. Endocrinol.* **145,** 543–559
2. Castro, A., Jerez, M. J., Gil, C., and Martinez, A. (2005) *Med. Res. Rev.* **25,** 229–244
3. Lerner, A., and Epstein, P. (2006) *Biochem. J.* **393,** 21–41
4. Wang, H., and Storm, D. R. (2003) *Mol. Pharmacol.* **63,** 463–468
5. Movsesian, M. A., and Bristow, M. R. (2005) *Curr. Top. Dev. Biol.* **68,** 25–48
6. Beavo, J. A., and Brunton, L. L. (2002) *Nat. Rev. Mol. Cell. Biol.* **3,** 710–718
7. Chin, K.-V., Yang, W.-L., Ravatn, R., Kita, T., Reitman, E., Vettori, D., Cvijic, M. E., Shin, M., and Iacono, L. (2002) *Ann. N. Y. Acad. Sci.* **968,** 49–64
8. Beavo, J. A. (1995) *Physiol. Rev.* **75,** 725–748
9. Houslay, M. D., and Milligan, G. (1997) *Trends Biochem. Sci.* **22,** 217–224
10. Hanoune, J., and Defer, N. (2001) *Annu. Rev. Pharmacol. Toxicol.* **41,** 145–174
11. Sunahara, R. K., and Taussig, R. (2002) *Mol. Interv.* **2,** 168–184
12. Hoffmann, R., Baillie, G. S., MacKenzie, S. J., Yarwood, S. J., and Houslay, M. D. (1999) *EMBO J.* **18,** 893–903
13. MacKenzie, S. J., Baillie, G. S., McPhee, I., Bolger, G. B., and Houslay, M. D. (2000) *J. Biol. Chem.* **275,** 16609–16617
14. MacKenzie, S. J., Baillie, G. S., McPhee, I., MacKenzie, C., Seamons, R., McSorley, T., Millen, J., Beard, M. B., van Heeke, G., and Houslay, M. D. (2002) *Br. J. Pharmacol.* **136,** 421–433
15. Sette, C., and Conti, M. (1996) *J. Biol. Chem.* **271,** 16526–16534
16. Zhao, A. Z., Huan, J.-N., Gupta, S., Pal, R., and Sahu, A. (2002) *Nat. Neurosci.* **5,** 727–728
17. Zaccolo, M., De Giorgi, F., Cho, C. Y., Feng, L., Knapp, T., Negulescu, P. A., Taylor, S. S., Tsien, R. Y., and Pozzan, T. (2000) *Nat. Cell Biol.* **2,** 25–29
18. Bos, J. L. (2003) *Nat. Rev. Mol. Cell. Biol.* **4,** 733–738
19. DiPilato, L. M., Cheng, X., and Zhang, J. (2004) *Proc. Natl. Acad. Sci. U. S. A.* **101,** 16513–16518
20. Nikolaev, V. O., Bunemann, M., Hein, L., Hannawacker, A., and Lohse, M. J. (2004) *J. Biol. Chem.* **279,** 37215–37218
21. Ponsioen, B., Zhao, J., Riedl, J., Zwartkruis, F., van der Krogt, G., Zaccolo, M., Moolenaar, W. H., Bos, J. L., and Jalink, K. (2004) *EMBO Rep.* **5,** 1176–1180
22. Boute, N., Jockers, R., and Issad, T. (2002) *Trends Pharmacol. Sci.* **23,** 351–354
23. Natarajan, M., Lin, K.-M., Hsueh, R. C., Sternweis, P. C., and Ranganathan, R. (2006) *Nat. Cell Biol.* **8,** 571–580
24. Steinhoff, M., Buddenkotte, J., Shpacovitch, V., Rattenholl, A., Moormann, C., Vergnolle, N., Luger, T. A., and Hollenberg, M. D. (2005) *Endocr. Rev.* **26,** 1–43
25. Pyne, S., and Pyne, N. (2000) *Biochem. J.* **349,** 385–402
26. Rosen, H., and Goetzl, E. J. (2005) *Nat. Rev. Immunol.* **5,** 560–570
27. Siehler, S., and Manning, D. R. (2002) *Biochim. Biophys. Acta* **1582,** 94–99
28. An, S., Zheng, Y., and Bleu, T. (2000) *J. Biol. Chem.* **275,** 288–296
29. Ancellin, N., and Hla, T. (1999) *J. Biol. Chem.* **274,** 18997–19002
30. Gonda, K., Okamoto, H., Takuwa, N., Yatomi, Y., Okazaki, H., Sakurai, T., Kimura, S., Sillard, R., Harii, K., and Takuwa, Y. (1999) *Biochem. J.* **337,** 67–75
31. Kon, J., Sato, K., Watanabe, T., Tomura, H., Kuwabara, A., Kimura, T., Tamama, K.-i., Ishizuka, T., Murata, N., Kanda, T., Kobayashi, I., Ohta, H., Ui, M., and Okajima, F. (1999) *J. Biol. Chem.* **274,** 23940–23947
32. Okamoto, H., Takuwa, N., Gonda, K., Okazaki, H., Chang, K., Yatomi, Y., Shigematsu, H., and Takuwa, Y. (1998) *J. Biol. Chem.* **273,** 27104–27110
33. Windh, R. T., Lee, M.-J., Hla, T., An, S., Barr, A. J., and Manning, D. R. (1999) *J. Biol. Chem.* **274,** 27351–27358
34. Nagai, T., Yamada, S., Tominaga, T., Ichikawa, M., and Miyawaki, A. (2004) *Proc. Natl. Acad. Sci. U. S. A.* **101,** 10554–10559
35. Singer, W., Miller, R., and Sternweis, P. (1994) *J. Biol. Chem.* **269,** 19796–19802
36. Griesbeck, O., Baird, G. S., Campbell, R. E., Zacharias, D. A., and Tsien, R. Y. (2001) *J. Biol. Chem.* **276,** 29188–29194
37. Rehmann, H., Das, J., Knipscheer, P., Wittinghofer, A., and Bos, J. L. (2006) *Nature* **439,** 625–628
38. Rehmann, H., Prakash, B., Wolf, E., Rueppel, A., de Rooij, J., Bos, J. L., and Wittinghofer, A. (2003) *Nat. Struct. Biol.* **10,** 26–32
39. Mandala, S., Hajdu, R., Bergstrom, J., Quackenbush, E., Xie, J., Milligan, J., Thornton, R., Shei, G.-J., Card, D., Keohane, C., Rosenbach, M., Hale, J., Lynch, C. L., Rupprecht, K., Parsons, W., and Rosen, H. (2002) *Science* **296,** 346–349
40. Osada, M., Yatomi, Y., Ohmori, T., Ikeda, H., and Ozaki, Y. (2002) *Biochem. Biophys. Res. Commun.* **299,** 483–487
41. Chen, J., DeVivo, M., Dingus, J., Harry, A., Li, J., Sui, J., Carty, D., Blank, J., Exton, J., Stoffel, R. H., Inglese, J., Lefkowitz, R. J., Logothetis, O. E., Hildebrandt, J. D., and Iyengar, R. (1995) *Science* **268,** 1166–1169
42. Tang, W. J., and Gilman, A. G. (1991) *Science* **254,** 1500–1503
43. Buhl, A. M., Johnson, N. L., Dhanasekaran, N., and Johnson, G. L. (1995) *J. Biol. Chem.* **270,** 24631–24634
44. Sah, V. P., Seasholtz, T. M., Sagi, S. A., and Brown, J. H. (2000) *Annu. Rev. Pharmacol. Toxicol.* **40,** 459–489
45. Brass, L. F., and Woolkalis, M. J. (1992) *Biochem. J.* **281,** 73–80
46. Haslauer, M., Baltensperger, K., and Porzig, H. (1998) *Mol. Pharmacol.* **53,** 837–845
47. Turner, J. T., Camden, J. M., Kansra, S., Shelton-James, D., Wu, H., and Halenda, S. P. (1992) *J. Pharmacol. Exp. Ther.* **263,** 708–716

Use of a cAMP BRET Sensor to Characterize a Novel Regulation of cAMP by the Sphingosine-1-phosphate/G_{13} Pathway

SUPPLEMENTAL DATA

Characterization of the CAMYEL sensor and calculation of intracellular concentrations of cAMP from BRET ratios. The purified sensor was used to determine the Kd and Hill coefficient for association of cAMP with the sensor; these were 8.8 μM and 1, respectively (Fig. S1). The response of the sensor to cAMP was independent of pH in the range of 6.5-8.0 and not affected by calcium at concentrations up to 1 mM (Fig. S2). The response time of the sensor was assessed by changes in BRET when the sensor was exposed to abrupt increases or decreases in cAMP. Such changes depend on both the association and dissociation of cAMP and the ensuing changes in conformation. *In vitro*, the change in BRET in response to altered cAMP appears to be complete in 1 to 2 seconds (Fig. S3). This rate of signal change is well suited for measuring the kinetics of change in intracellular concentrations of cAMP.

Ratiometric data was converted to cAMP concentration using the equation:

$$[\,cAMP\,] = Kd * \{\frac{(R - R\ \min)}{(R\ \max - R)}\}$$

The Kd and n are 8.8 μM and 1, respectively (Fig. S1). R is the intensity ratio of RL to YFP. Rmax was obtained by adding 2 mM 8-Bromo cAMP to the cells at the end of the assay (Fig. 2*B*). An identical Rmax value can be obtained by lysing the cells with 0.1% NP-40 and adding a saturating amount of cAMP (2 mM) at the end of the assay. At this time an absolute value for Rmin can not be determined. However, the basal cAMP concentration in RAW 264.7 cells is very low and estimated to be in the range of 40-100 nM based on measurements of total cellular cAMP with the EIA and cell volume. The difference in BRET ratio at this concentration of cAMP vs. no cAMP falls within the error of our measurements. In addition, treatment with inhibitors of phosphodiesterases does not significantly alter basal cAMP in the cells as measured by both EIA and the CAMYEL sensor. Therefore, we arbitrarily set Rmin to be the average ratio of measurements with unstimulated cells minus 4 standard deviations. This ensures that Rmin is always less than the measured value. Note: measurements of total intracellular cAMP by EIA in unstimulated cells yield ~2 pmol/mg protein. The RAW 264.7 cells contain about 1mg protein per 10^7 cells and the cell volume was estimated by microscopy to be 2-5 pL. According to these numbers the basal intracellular concentration of cAMP is estimated to be 40-100 nM, much of it presumably bound to intracellular proteins.

The validity of these calculations is supported by the fact that the Rmax to Rmin ratio calculated from live cell assays is the same as ratios for purified proteins and that the calculations for cAMP in stimulated samples are proportionally in agreement with the results from the EIA. In Figure 3*A*, a baseline BRET ratio of 1.53, which represents essentially unliganded sensor, could be stimulated to 2.61 when cells were saturated with 8-Bromo cAMP, an increase of about 70%. This magnitude of change is similar to what we observed with the purified protein in response to cAMP (Figure 1*C*). In Figure 3*B*, the ratios between various ligand-induced cAMP responses appear to be similar to those observed with the EIA as well. Finally, we determined the concentration-response relationships for ISO and S1P (Fig. S4). The EC_{50} for ISO was about 20 nM either in the presence or absence of S1P; the EC_{50} for S1P in the presence of 16 nM ISO was about 8 nM. These results are also similar to those determined by EIA. Based on these comparisons, we believe this approach to convert ratiometric measurements to actual concentrations of cAMP is valid.

Independent validation of G_{13} involvement in the S1P synergy on cAMP. Knockdown of $G\alpha_{13}$ using siRNA greatly reduced the S1P enhancement on cAMP synthesis as measured with the CAMYEL sensor. To independently validate the involvement of $G\alpha_{13}$, we used a micro-RNA based shRNA delivered via retroviral infection to knockdown $G\alpha_{13}$. The targeting sequence is 5'-TGGGTGAGTCTGTAAAGTA-3', which was independently selected from the siRNA sequences. In addition, we measured the

cAMP response using the EIA method. As shown in Supplementary Figure S5, the cAMP response to ISO and S1P was attenuated, while the response to ISO alone or ISO and UDP remained unchanged.

Rho GTPase is not involved in the S1P enhancement on cAMP synthesis. Well-characterized downstream effectors of the G_{13} pathway are the Rho GTPases, which can mediate cytoskeleton rearrangement during chemotaxis, cell adhesion, phagocytosis and cell cycle progression (43,44). To assess the involvement of Rho proteins in the S1P effect on cAMP synthesis, we applied *Clostridium difficile* toxin B and a Rho kinase inhibitor, H1152, to block Rho and Rho kinase activity, respectively. As shown in figure S6*A*, none of the inhibitors affected the ability of S1P to enhance cAMP synthesis. The effectiveness of *C. difficile* toxin B to block activation of Rho was verified by direct assessment of the activated GTPase in response to S1P (Fig. S6*B*). Therefore, the synergistic effect of S1P on cAMP synthesis does not appear to involve Rho.

The synergistic effect of S1P on cAMP exists in primary macrophages. To explore the physiological relevance of the S1P synergism on cAMP, we examined the cAMP responses in primary bone marrow-derived macrophage (BMDM) cells. Not surprisingly this synergism is more profound in the BMDM cells, where addition of S1P boosted the production of cAMP triggered by ISO or PGE over 10-fold (Fig. S7). In these primary cells the synergistic effect was also more prolonged, lasting throughout the 5-minute period of assessment.

SUPPLEMENTAL EXPERIMENTAL PROCEDURES

Reagents. Clostridium difficile toxin B and H1152 were purchased from Calbiochem.

Assay of activated Rho. Cells ($1x10^6$) were plated on 60 mm tissue culture dishes one day prior to the assay. On the day of assay, cells were cultured in serum-free medium with or without 10 ng/ml *Clostridium difficile* toxin B for 1 hour. Ligands were then added to stimulate the cells. Reactions were stopped after 1 minute of stimulation by rapid removal of medium and placement on ice; the cells were immediately washed with ice-cold 1xPBS and lysed with 200 μl lysis buffer. Cell lysates were cleared by brief centrifugation and assayed using the G-LISA RhoA activation assay kit (Cytoskeleton Inc.).

Isolation of BMDM. Bone marrow derived primary macrophages were isolated from mouse femurs and cultured as described (49).

SUPPLEMENTAL REFERENCE

49. Takeshita, S., Kaji, K., and Kudo, A. (2000) *J Bone Miner Res.* **15**, 1477-1488

SUPPLEMENTAAL FIGURE LEGANDS

Figure S1. Concentration dependence of BRET changes induced by cAMP or 8-Bromo-cAMP. Data plotted are averages of 3 experiments. Bacterial expressed protein with an N-terminal 6xHis tag was purified with Ni-NTA resin. Protein was diluted to 20 nM with buffer containing 20 mM NaHEPES, pH 7.4, 50 mM KCl, 50 mM NaCl, 2.5 mM $MgCl_2$, 0.2% NP-40, 5 mM DTT, protease inhibitors, and mixed with the indicated concentrations of the cyclic nucleotide and 2 μM coelenterazine-h before assay. The BRET signal was measured by simultaneous measurements at wavelengths of 475 nm and 535 nm using a POLARstar Optima. The BRET ratio is expressed as RL/YFP (475/535). The maximal change in BRET was similar for cAMP and 8-Bromo cAMP. When the Hill function equation was used to fit the data, a Kd for cAMP of 8.8 +/- 0.6 μM, a Kd for 8-Bromo cAMP of 1.8 +/- 0.2 μM and Hill coefficients of 0.97 and 1.07, respectively, were obtained.

Figure S2. The BRET ratio of CAMYEL sensor is not affected by changes in calcium concentration or pH. CAMYEL protein was diluted to 20 nM with buffer containing 20 mM NaHEPES, 50 mM KCl, 50 mM NaCl, 2.5 mM $MgCl_2$, 0.2% NP-40, 5 mM DTT, and protease inhibitors, at the indicated pH or with 1mM calcium. The BRET signal was measured in the presence of 2 μM coelenterazine-h substrate with or without 100 μM cAMP. The BRET ratio is expressed as RL/YFP (475/535).

Figure S3. Kinetics of cAMP-induced changes in BRET with the CAMYEL sensor protein. For measuring the kinetics of cAMP binding and associated changes in BRET, 50 μl of 20 nM CAMYEL protein was added to a well on a 96 well plate in the presence of 2 μM coelenterazine-h and RL/YFP ratios were measured using a POLARstar Optima. At the time indicated by the arrow, 2x cAMP was injected into the well at 420 μl per second to reach the indicated final cAMP concentration. For measuring the BRET changes induced by dissociation of cAMP from the CAMYEL protein, 30 μl of 50 nM CAMYEL protein was added to a well on a 96 well plate in the presence of the indicated cAMP concentration and 5 μM coelenterazine-h and RL/YFP ratios were measured. At the time indicated by the arrow, 210 μl of buffer was injected into the well at 420 μl per second to reach the indicated final concentration of cAMP (1/8 of the initial concentration).

Figure S4. Concentration response curves of RAW 264.7 cells as measured with the CAMYEL sensor. ***A,*** RAW cells expressing CAMYEL were stimulated with the indicated concentrations of S1P in the presence of 16 nM ISO. ***B,*** RAW cells expressing CAMYEL were stimulated with the indicated concentrations of ISO in the absence or presence of 10 nM S1P. The percent max peak response was calculated as the peak response divided by maximal peak response observed times 100. Data shown are averages of 3 experiments.

Figure S5. G_{13} mediates the S1P synergy on cAMP as measured by EIA. RAW cells were infected with retrovirus expressing micro-RNA targeting $G\alpha_{13}$ or non-targeting sequences (control). At time 0, cells were stimulated with 50 nM ISO (***A***), 50 nM ISO and 25 μM UDP (***A***), or 50 nM ISO and 1 μM S1P (***B***) as indicated. At the given times reactions were stopped by removal of medium and addition of cell lysis solution and cAMP was determined by EIA. Error bars represent the standard deviation of results from 5 independent experiments.

Figure S6. Inhibition of Rho activation did not affect the enhancement of cAMP responses by S1P. ***A,*** Cells were pretreated with 10 ng/ml *Clostridium difficile* toxin B (TxB) for 1 hour or 10 μM H1152 for 30 minutes prior to assay. Cells were stimulated with 16 nM ISO followed by 10 nM S1P at times indicated by the arrows. Intracellular cAMP was measured with the CAMYEL sensor. Error bars represent the standard deviation of results from 4 experiments. ***B,*** Effectiveness of TxB treatment. Cells were

pretreated with TxB as described above followed by stimulation with 1 μM S1P. The reactions were stopped at 1 minute and cells were lysed and assayed for Rho activation using the G-LISA kit. Error bars represent the standard deviation of results from 3 experiments.

Figure S7. Changes in cAMP in BMDM cells. At time 0, cells were stimulated with 16 nM ISO, 16 nM ISO and 10 nM S1P, 10 μM PGE, 10 μM PGE and 10 nM S1P, or 50 nM S1P as indicated. At the given times reactions were stopped by removal of medium and addition of cell lysis solution and cAMP was determined by EIA. The results shown are the average of 3 independent experiments done with two different preparations of cells: the variance among the experiments is about 30% of the signals.

Supplementary Figure S1

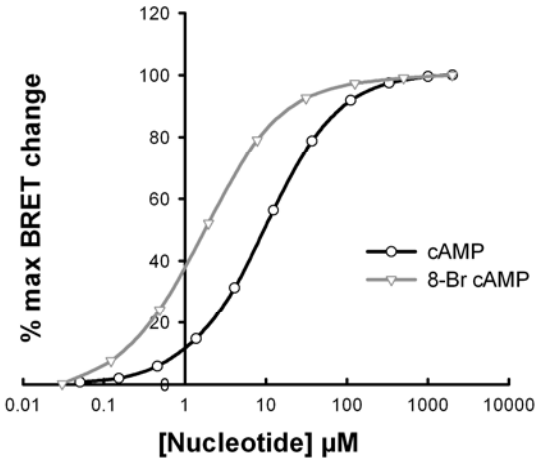

Supplementary Figure S2

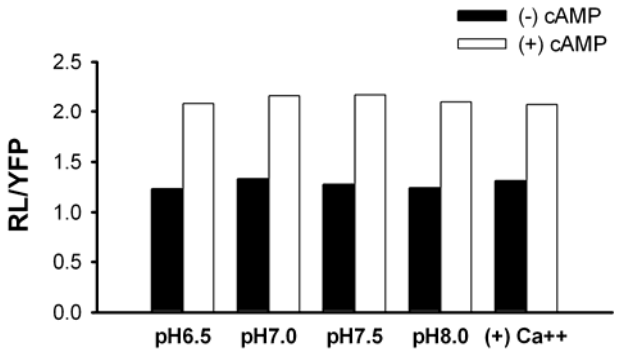

Supplementary Figure S3

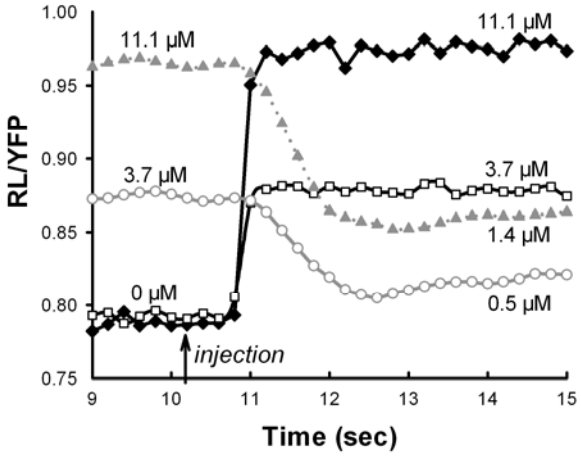

Supplementary Figure S4

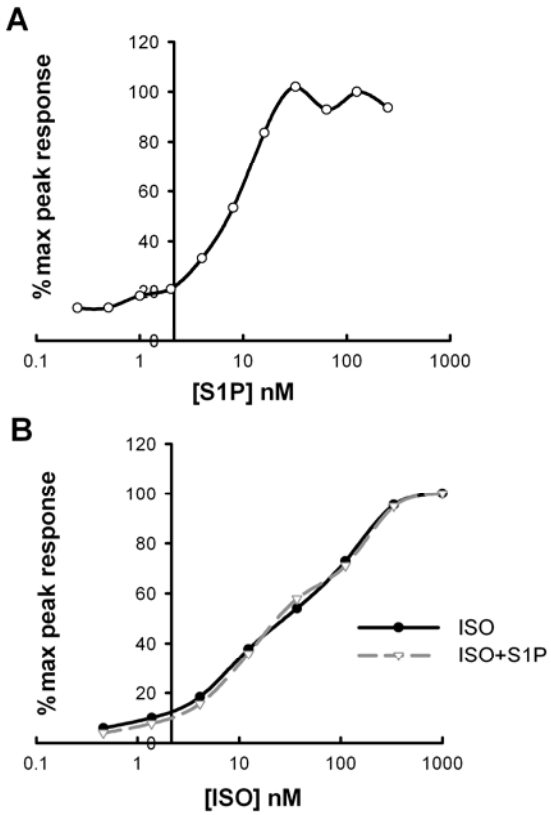

Supplementary Figure S5

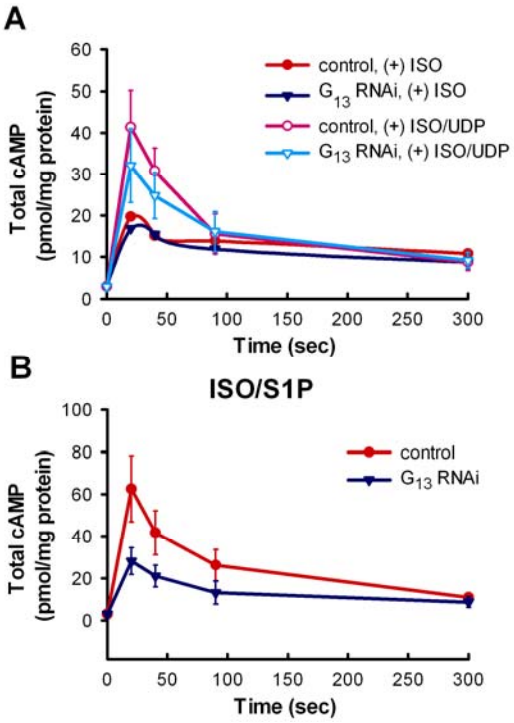

cAMP BRET sensor reveals G_{13} regulation of cAMP

Supplementary Figure S6

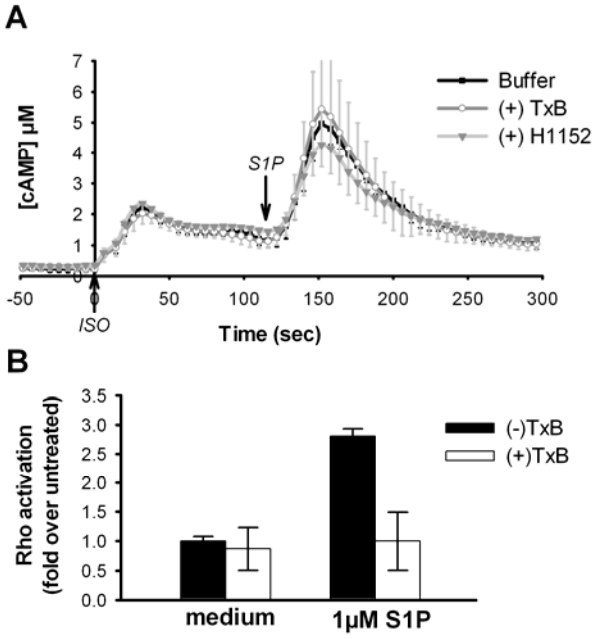

Supplementary Figure S7